

Annual cycle of energy balance of Zongo Glacier, Cordillera Real, Bolivia

Patrick Wagnon¹, Pierre Ribstein², Bernard Francou³, and Bernard Pouyaud⁴

Abstract. An 18-month meteorological data set recorded at 5150 m above sea level (asl) on Zongo Glacier, in the tropical Andes of Bolivia, is used to derive the annual cycle of the local energy balance and to compare it to the local mass balance. The roughness parameters needed to calculate the turbulent fluxes over the surface are deduced from direct sublimation measurements performed regularly on the field site and serve as calibration parameters. For the hydrological year September 1996 to August 1997, net all-wave radiation (16.5 W m^{-2}) is the main source of energy at the glacier surface and shows strong fluctuations in relation to the highly variable albedo. An important peculiarity of tropical glaciers is the negative latent heat flux (-17.7 W m^{-2}) indicating strong sublimation, particularly during the dry season. The latent heat flux is reduced during the wet season because of a lower vertical gradient of humidity. The sensible heat flux (6.0 W m^{-2}), continuously positive throughout the year, and the conductive heat flux in the snow/ice (2.8 W m^{-2}) also bring energy to the surface. There is a good agreement between the monthly ablation calculated by the energy balance and the ablation evaluated from stake measurements. The seasonality of the proglacial stream runoff is controlled by the specific humidity, responsible for the sharing of the energy between sublimation and melting.

1. Introduction

A glaciological program has been undertaken on Zongo Glacier, Cordillera Real, Bolivia (16°S , 68°W) since 1991. This program involving mass balance measurements [Francou *et al.*, 1995], hydrological studies [Ribstein *et al.*, 1995], and energy balance investigations [Wagnon *et al.*, 1998] aims at improving our knowledge about the functioning of tropical glaciers. This paper describes the annual cycle of the energy fluxes over Zongo Glacier surface at the altitude of the mean equilibrium line (5150 m above sea level (asl)). These fluxes are derived from meteorological measurements collected by an automatic weather station. Knowledge of the specific characteristics of this glacier (for example, surface state, wind regimes, surface temperatures) was obtained during various few-day field surveys chosen in the dry or the wet season. These field trips, where direct measurements of sublimation were performed, were crucial for obtaining the roughness parameters.

Very few energy balance studies have been conducted in low latitudes. Some work on radiation budget has been undertaken on Lewis Glacier, Mount Kenya [Hastenrath and Patnaik, 1980; Hastenrath and Kruss, 1988], and on Quelccaya ice cap, Peruvian Andes [Hastenrath, 1978], but no annual cycle energy balance studies have yet been processed. Interesting interpretations of the mass balance fluctuations of Mount Kenya's glaciers [Hastenrath

and Kruss, 1992] and of Yanamarey Glacier, Cordillera Blanca, Peru [Hastenrath and Ames, 1995] have been proposed in terms of energy balance changes. Unfortunately, these studies lacked well-documented long-term energy balance measurements. Such works have already been conducted over Antarctic blue ice [Bintanja *et al.*, 1997] or over a winter snow cover in the Sierra Nevada (United States) [Marks and Dozier, 1992], but they have never yet been done on a tropical glacier. The results will be discussed in order to underline the specific characteristics of Bolivian glaciers.

The energy balance plays a key role in the understanding of snowmelt seasonality and thus the variations of the proglacial stream runoff with seasons. The accumulation season between October and March coincides with the period of higher ablation and melt rates at the glacier surface, which leads to high discharges of the stream escaping from the glacier snout. However during the dry season (May-August) the absence of precipitation is compensated by a reduced but permanent ablation with low discharges of the proglacial stream.

2. Location and Measurement Program

The glacier is located in the Huayna Potosi Massif (Cordillera Real, Bolivia), at $16^{\circ}15' \text{ S}$, $68^{\circ}10' \text{ W}$, on the western margin of the Amazon Basin, approximately 30 km north of La Paz. This valley-type glacier is 3 km long and has a surface area of 2.1 km^2 . A map of this glacier and a precise location are given in Figure 1. The upper reaches are exposed to the south, whereas the lower section surrounded by two steep lateral moraines faces east. The maximum and minimum elevations are 6000 and 4900 m asl, respectively. The altitude of the equilibrium line under steady state conditions (annual mass balance approaching zero) is 5150 m asl. The Zongo Glacier is part of a 3 km^2 basin (77% glacierized) above the main hydrometric station located at 4830 m asl (Figure 1).

Although the first equipment was installed in July 1991 (glaciological stakes, hydrometric station, rain gauges,

¹Laboratoire de Glaciologie et de Géophysique de l'Environnement, Saint Martin d'Hères, France.

²Institut Français de Recherche Scientifique Pour le Développement en Coopération (ORSTOM), Paris VI, France.

³ORSTOM, Quito, Ecuador.

⁴ORSTOM, La Paz, Bolivia.

Copyright 1999 by the American Geophysical Union.

Paper number 1998JD200011.

0148-0227/99/1998JD200011\$09.00



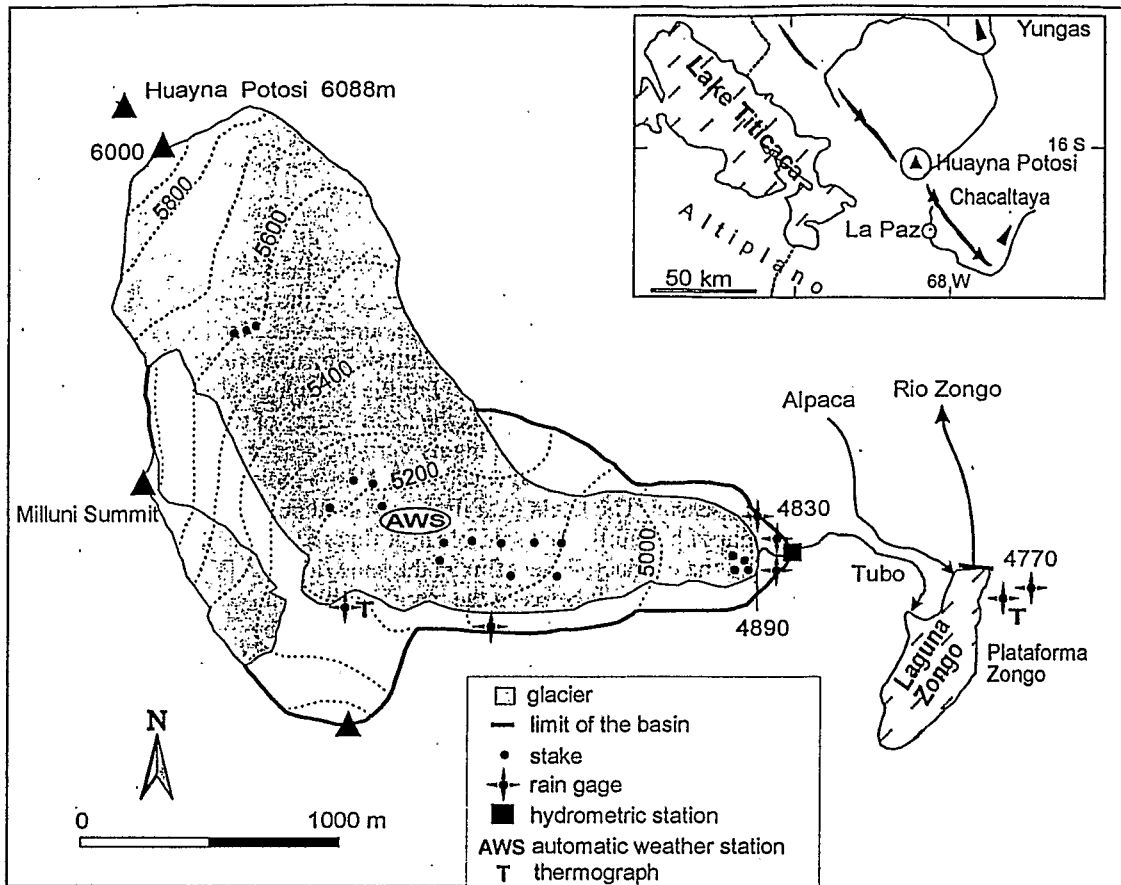


Figure 1. A simplified orientation map of Zongo Glacier (2.1 km²) showing location of monitoring equipment.

thermograph), the definitive automatic energy budget station has been running since March 1996. This automatic weather station is located close to the axis of the glacier, at 5150 m asl on a relatively flat area (Figure 1) and is checked every 10 days. The station faces southeast and is in sunlight as soon as the Sun rises, but it is in shade after the middle of the afternoon between 1530 and 1600 LT, depending on the season.

The measurements are made within the boundary surface layer using sensors manufactured by Campbell (United Kingdom). Ventilated dry and wet bulb temperatures, wind speed, and direction are recorded as halfhourly means over 15-s time steps at two levels above the glacier surface (usually 0.3 and 1.8 m above the surface, depending on the ablation or accumulation; the zero-reference level is the mean height of the surface obstacles). Moreover, incident and reflected short-wave radiations (usually 1 m above the surface), net all-wave radiation (usually 1 m above the surface), and temperatures at various depths inside the snow/ice are recorded as halfhourly means over 15-s time steps. The heights (or depths) of the sensors may vary with ablation or accumulation of snow, but thanks to an ultrasound sensor (Campbell UDG01 ultrasonic depth gauge, accuracy: ± 1 cm), these heights are known with precision every day. Dry and wet bulb temperatures are obtained from psychrometers equipped with Cu-Cst thermocouples and ventilated permanently by a motor whose energy supply comes from a truck battery (12V/100Ah), loaded by a 43 W solar panel. Air is aspirated at the top of the psychrometer at a constant speed of 4 m s⁻¹. To prevent measurement errors due to radiation, these psychrometers are shielded with two white interlocked cylinders of 8 and 12 cm

diameters, topped by a white 30-cm diameter disk. Campbell Met One and Young anemometers provide wind speed and direction. Li-Cor and SP1100 pyranometers ($0.35 < \lambda < 1.1 \mu\text{m}$) provide short-wave radiation, and a Q-6 net radiometer ($0.25 < \lambda < 60 \mu\text{m}$) provides net all-wave radiation. Snow/ice temperatures are given by Cu-Cst thermocouples soldered on 5 cm x 5 cm white metallic squares in order to avoid conductive warming of the sensor through the wire, from the surface. Five thermocouples were originally put in snow at 20, 30, 50, 70, and 100 cm depth inside horizontal white 40 cm high cylinders of 30 cm diameter, used as screens against solar radiation. Two other thermocouples were installed in ice originally at 1.5 and 2.7 m depth, without being shielded from solar radiation. In March 1996, most of these sensors were new and adequately calibrated prior to the installation of the energy budget station on the glacier. In addition to accuracy tests by the manufacturer, intercomparisons of the sensors of the station and with other available sensors (Q-7 Campbell net radiometer or handle psychrometer for example) have been carried out before their use on the glacier and while they were running at the weather station. The accuracy of the sensors is estimated according to these intercomparisons and the manufacturer's specifications. Table 1 gives a list of the sensors of this Campbell station, with their specificity. Excluding gaps due to data logger breakdowns, the entire data set comprises 521 days from March 29, 1996 to October 15, 1997.

To improve our knowledge and understanding of the local climatic conditions to increase the accuracy of energy flux calculations, several few-day field trips were conducted on the field site. These field trips corresponded to the dry season (August

Table 1. List of Different Sensors With Their Specificity, Installed on the Weather Station at 5150 m Above Sea Level (asl)

Quantity	Sensor Type	Height, cm	Accuracy
Air temperature, °C	Cu-Cst thermocouples	30 and 180	±0.3°C
Vapor pressure, hPa	Wet bulb Cu-Cst thermocouples	30 and 180	±0.3 hPa
Wind speed, m s ⁻¹	Met One Campbell -Campbell 05103-Young	30 and 180	±1.5%
Wind direction, deg	Campbell 05103-Young	30 and 180	±3 deg
Incident short-wave radiation, W m ⁻²	Campbell SP1100 and Li-Cor	100	±3%
Reflected short-wave radiation, W m ⁻²	Campbell SP1100 and Li-Cor	100	±3%
Net all-wave radiation, W m ⁻²	Q-6 net radiometer	100	from ±3% to ±10%
Snow/ice temperature, °C	Cu-Cst thermocouples	-20, -30, -50, -70, -100, -150, -270	±0.3°C

22-28, 1996; May 19-27, 1997; and July 31 to August 12, 1997) and also to the wet season (November 13-18, 1996; March 1-8, 1997; and October 1-10, 1997). As many qualitative observations as possible were made during these days to describe the wind regimes, the weather types, the surface state, the hours of beginning of surface melting or refreezing, the cloud types. The cloudiness was estimated regularly every 15 min during the day, every 2 hours at night. Surface temperatures were also measured every 2 hours using 5 Pt thermistors, soldered on 5 cm x 5 cm white metallic squares. These Pt probes laid down right at the surface of the snow/ice. Because they were not shielded from radiation, they regularly showed positive values during the day, which is inconsistent. Nevertheless, at night, these sensors agreed fairly well with each other, and the accuracy of the surface measurement is supposed to be ± 0.5°C. During the day, the surface temperature is set to 0°C as soon as melting is observed. Every 24 hours, sublimation was measured using lysimeters which consist in translucent plastic pails of 165 cm² surface (round type) or 395 cm² surface (square type) and 10 cm deep. The 10 lysimeters (7 round and 3 square ones) were buried 10 cm into the snow/ice and were filled with snow/ice. The natural surrounding surface was then reconstructed as well as possible. After a few hours, snow metamorphism had occurred and lysimeter surface was believed to be totally representative of natural surfaces. They were weighed with an accuracy of ± 1 g corresponding to ± 0.061 mm for the round lysimeters or ± 0.025 mm for the square lysimeters. Daily values of sublimation were sufficiently high to be obtained by this simple device as shown by the good agreement between all the lysimeters. During days with snowfall, sublimation was impossible to measure, and it was assumed to be zero during precipitation events. Direct measurements of sublimation are very scarce during the wet season. Ablation/accumulation was measured on the site using a network of 12 white Polyvinylchloride (PVC) ablation stakes, measured every morning and evening. Snow density was measured at the same time with a 550 cm³ metallic cylinder and an accurate weighing machine. Daily melting was obtained with a so-called "fusion box," composed of a double white 50 cm x 50 cm square box. The inner box (15 cm deep), the bottom of which is made of three superposed layers of grid (1 mm x 1 mm), is filled with snow/ice

making sure that the natural surrounding surfaces were reconstructed as well as possible. When melting occurs, water percolates through the snowpack and is collected in the outer waterproof box (20 cm deep). This fusion box is buried 20 cm into the snow, and the total mass of collected water is weighed every morning with accuracy, giving the daily melting of the day before. Since March 1997, during these field trips, more detailed vertical profiles of ventilated air temperature (Cu-Cst thermocouples) were also available, from another Campbell data logger recording mean data every 5 min over 5-s time steps. Seven sensors were localised at 0, 10, 20, 30, 40, 50, and 100 cm above the glacier surface, and they were shielded from radiation. The reference temperature for the thermocouples was obtained from a liquid water-ice bath at 0°C. Accuracy is ± 0.3°C. While we were on the field site, the air pressure did not vary much, and we took the constant value of 540 hPa for the entire measuring period.

3. Climatic Conditions

The Zongo Glacier belongs to the outer tropics, as defined by Kaser [1996]. The climate is determined by homogeneous air masses and by seasonal oscillation of the intertropical convergence zone (ITCZ). Between May and August the ITCZ is north of Bolivia and tropical anticyclones produce a pronounced dry season, whereas from October to March, the ITCZ proceeds to its most southerly position. This is the wet season coinciding with the eastern intertropical flux that brings water vapor from the Atlantic [Roche *et al.*, 1990]. Figure 2 shows the daily precipitation for four hydrological years (from September 1 to August 31) at 4770 m asl in the Zongo valley approximately 1 km from the glacier tongue. Around 85% of the total annual precipitation falls during the wet season (October-March).

Figure 3 shows the temporal variation in some meteorological quantities during the entire measuring period. Table 2 summarizes the annual mean values and extremes (based on daily averaged values) of the meteorological parameters for the entire hydrological year 1996-1997 (September 1 to August 31) and for both seasons. Another peculiarity of the tropical climate is the very low thermal seasonality. Indeed, the diurnal and annual range of temperature are approximately equal with an annual temperature amplitude which does not exceed 9°C (based on daily averaged values). In such conditions the terms of winter and summer are inappropriate to describe this outer tropic climate, and as A. von Humboldt said, "the night is the winter of the tropics." The largest variations in air temperature occur during the dry season, when there are fluctuations of 7°C within a few days. The temperatures of the wet season are slightly higher than those of the dry season with respective means of -0.2°C and -3.8°C (Table 2). Disregarding short-term fluctuations, relative humidity is fairly constant throughout the year, with slightly lower values during the dry season. Specific humidity shows a more pronounced seasonality with higher values during the wet season than during the dry one (mean values are 5.8 and 4.4 g kg⁻¹, respectively). The wind speed is low on the site but is highly variable within a few days. On Zongo Glacier, we observe preferentially two typical wind regimes: at night the radiational cooling favors katabatic winds with a direction of 300° and by day, advected air masses invade the glacier from downward in the eastern direction. Night katabatic winds are slightly stronger during the dry season, with peaked values reaching 7 m s⁻¹, than during the wet season (respective means are 2.9 and 1.9 m s⁻¹). This is due to the fact that nocturnal cloudiness of the dry season is always zero, and hence

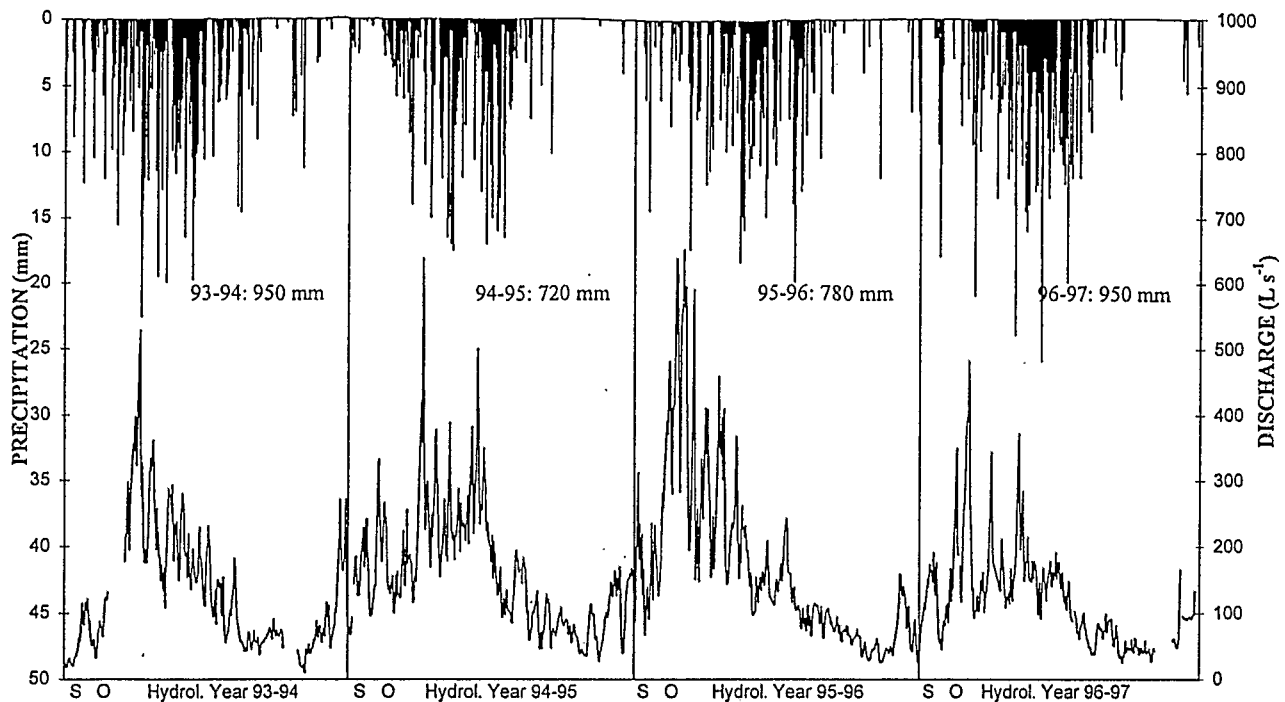


Figure 2. Daily precipitation recorded at 4770 m asl, 130 m below the glacier tongue (histograms), and daily discharge of the proglacial stream recorded at the limnometric station at 4830 m asl (line) (September 1993 to August 1997).

radiational cooling is higher, which leads to stronger katabatic winds. Figure 4 shows daily means of net all-wave radiation, incident short-wave radiation, and every day instantaneous minima of albedo. Albedo is highly variable with seasons with high values during the wet season due to fresh snow accumulating on the glacier almost every day. On the other hand, as soon as the dry season starts, albedo decreases slowly while the snow surface gets dirtier, while snow turns into firn and ice, and while penitents develop at the surface (old-snow spikes regularly distributed at the glacier surface). This slow decrease of the albedo is occasionally perturbed by peaked values corresponding to sporadic snow storms. The deposited fresh snow usually melts within a few days, and the albedo returns to its value prior to the storm. Neither net radiation nor solar radiation present any pronounced seasonality. Indeed, if short-term fluctuations are disregarded, solar radiation is fairly constant throughout the year. Net radiation is more variable, but no constant trend from year to year can be drawn. Usually, the glacier surface receives the same amount of net all-wave radiation during the dry or the wet season (Table 2): the more positive short-wave radiation budget of the dry season due to lower albedo is compensated by a more negative long-wave radiation budget due to very reduced cloudiness. The months of August and September 1996 present very high values of net all-wave radiation. This unusual pattern is explained by an extremely icy and dirty surface of the field site (minimum albedo reaching 0.2) more typical of the glacier tongue than of the mean equilibrium line area.

Another peculiarity of Bolivian glaciers is the presence of penitents during the dry season. The required weather conditions, sunny, dry, and moderately cold weather [Lliboutry, 1954, 1964; Kotlyakov and Lebedeva, 1974], are gathered on Zongo Glacier during the dry season, and penitents usually appear at the surface in the course of June. They may reach 40 or 50 cm height by the end of July at the field site (Figure 5). In August the meltwater

streaming at the surface makes them collapse, or they are partly buried by snow during storms.

A limnometric station located at 4830 m asl records instantaneous discharge of the proglacial stream escaping from the glacier snout. Figure 2 shows the hydrograph of the stream based on daily averaged values, for four hydrological years. In the outer tropics, ablation occurs throughout the year which is another important peculiarity of Bolivian glaciers. Nevertheless, disregarding short-term fluctuations, the runoff of Zongo Glacier shows an appreciable seasonal variability, with low discharges in the dry season and high values in the humid season. Table 3 summarizes the discharge mean values for the entire year, and for both seasons: the runoff of the wet season is usually 3 times higher than during the dry season. Therefore the accumulation season is concomitant with the period when ablation is the strongest. The mean annual discharge of the hydrological year 1996-1997 which is of interest in this study is 122 L s^{-1} , the lowest of the four presented cycles.

Subject to climatic conditions drastically different from midlatitude or polar glaciers, Bolivian glaciers have a peculiar behavior with a permanent and highly seasonal ablation. Nevertheless, most of the meteorological quantities like net all-wave radiation or air temperature are fairly constant throughout the year and cannot explain this runoff seasonality. Therefore a precise energy balance investigation is necessary to get a good insight into the specific metabolism of these glaciers.

4. Energy Balance Study

An energy balance study for the period March 1996 to October 1997 is presented. If we ignore horizontal energy transfers and define the volume from the surface to a depth where there is no significant heat flux, the energy balance of a snowpack may be written as [Oke, 1987]

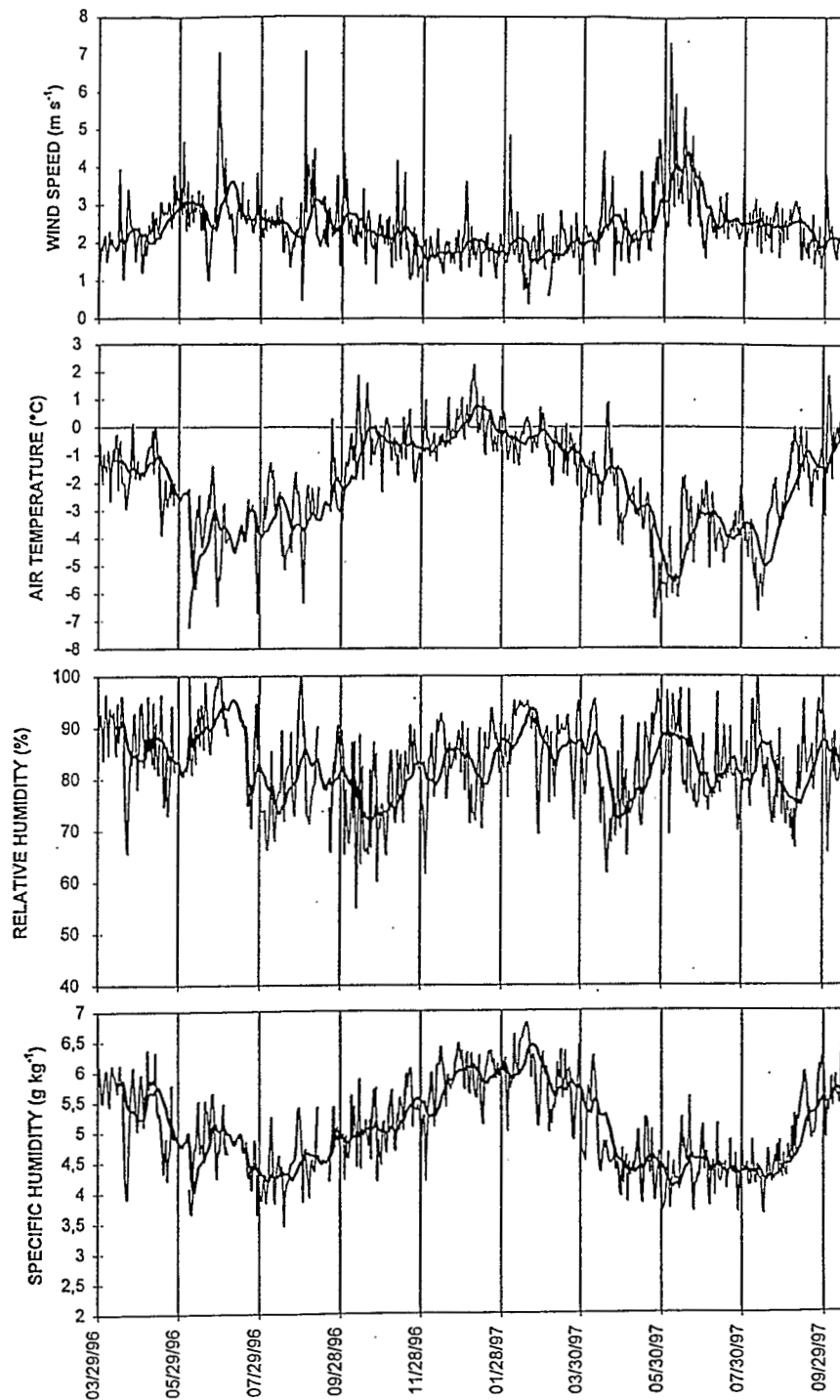


Figure 3. Variation in the daily mean values of wind speed, air temperature, relative humidity, and specific humidity over the entire measuring period from March 29, 1996 to October 15, 1997, measured at 30 cm above the glacier surface, at 5150 m asl. The thick line is the 15-day running mean.

$$R + H + LE + G + P = \Delta Q_M + \Delta Q_S \quad (1)$$

where R is net all-wave radiation, H is the turbulent sensible heat flux, LE is the turbulent latent heat flux, G is the conductive energy flux in the snow/ice, P is the heat supplied by precipitation, ΔQ_M is the latent heat storage change due to melting or freezing, and ΔQ_S is the convergence or divergence of sensible heat fluxes within the snowpack volume. Energy fluxes directed toward the surface are defined as positive and those from the

surface negative. Since precipitation is always snow in the vicinity of the equilibrium line and since snowfall intensities are usually weak, P remains insignificant and negligible as compared to the other terms of this equation (1).

4.1. Net All-Wave Radiation

The net radiation is the balance of the incident and reflected short-wave radiation and the incident and emitted long-wave radiation.

Table 2. Mean and Extreme (Based on Daily Averages) Meteorological Data for Hydrological Year 1996-97 and for Both Wet and Dry Seasons of This Year, Measured at 30 cm Above Glacier Surface

Quantity	Sept. 96 to Aug. 97			Nov. 96 to Feb. 97			May 97 to Aug. 97		
	Min	Mean	Max	Min	Mean	Max	Min	Mean	Max
$T, ^\circ\text{C}$	-6.93	-1.83	2.25	-2.00	-0.25	2.25	-6.93	-3.83	-1.87
$u, \text{m s}^{-1}$	0.36	2.36	7.34	0.36	1.88	4.86	1.46	2.85	7.34
RH, %	54.9	82.2	100	61.4	83.9	95.2	65.1	82.7	97.3
$q, \text{g kg}^{-1}$	3.63	5.08	6.80	4.18	5.79	6.80	3.69	4.37	5.22
$R, \text{W m}^{-2}$	-27.1	16.1	131.0	-21.7	12.7	109.2	-27.1	10.5	55.7
$S, \text{W m}^{-2}$	86.4	211.3	369.2	108.0	196.3	340.3	86.4	219.7	289.7
α, min	0.21	0.58	0.86	0.22	0.66	0.81	0.31	0.52	0.85

T is temperature, u is wind speed, RH is relative humidity, q is specific humidity, R is net all-wave radiation, S is incident short-wave radiation, and α, min is the daily minimum of albedo.

$$R = S\downarrow(1-\alpha) + L\downarrow - L\uparrow \quad (2)$$

where $S\downarrow$ is the incident short-wave radiation, α is the short-wave albedo of the snow/ice surface, $L\downarrow$ is the incident long-wave radiation, and $L\uparrow$ is the emitted long-wave radiation. The net all-wave radiation is measured directly on the field site by a Q-6 Campbell net radiometer ($0.25 < \lambda < 60 \mu\text{m}$). The accuracy of this sensor depends on its horizontality, which was controlled continuously while we were on the field site and every 10 days the rest of the time.

4.2. Turbulent Fluxes

4.2.1. Monin-Obukhov similarity theory. The transport of heat and moisture in the surface boundary layer of the atmosphere is dominated by turbulent motions. The turbulent sensible and latent heat fluxes can be calculated with the Monin-Obukhov similarity theory. According to this theory the mean vertical gradients of wind speed $v = (u, v)$, potential temperature θ , and specific humidity q are related to the corresponding fluxes as

$$\frac{kz}{u^*} \frac{\partial u}{\partial z} = \Phi_m \left(\frac{z}{L} \right) \quad (3)$$

$$\frac{kz}{\theta^*} \frac{\partial \theta}{\partial z} = \Phi_h \left(\frac{z}{L} \right) \quad (4)$$

$$\frac{kz}{q^*} \frac{\partial q}{\partial z} = \Phi_v \left(\frac{z}{L} \right) \quad (5)$$

The characteristic scales of velocity u^* (also called the friction velocity) of potential temperature θ^* and of specific humidity q^* are defined by

$$u^* = (\tau / \rho)^{1/2} \quad (6)$$

$$\theta^* = H / (\rho C_p u^*) \quad (7)$$

$$q^* = LE / (\rho L_s u^*) \quad (8)$$

where τ is the surface stress, $\rho = 0.69 \text{ kg m}^{-3}$ is the air density at 5150 m asl (540 hPa), C_p is the specific heat capacity for air at constant pressure ($C_p = C_{pd} (1 + 0.84q)$ with $C_{pd} = 1005 \text{ J kg}^{-1} \text{ K}^{-1}$, the specific heat capacity for dry air at constant pressure), L_s is the latent heat of sublimation of snow/ice ($L_s = 2.834 \cdot 10^6 \text{ J kg}^{-1}$), z is the height above the surface, and k is the von Karman constant ($k=0.4$). The nondimensional stability functions for momentum (Φ_m), for heat (Φ_h), and moisture (Φ_v) have to be determined

empirically and are assumed to depend only on the stability parameter z/L , where L is the Monin-Obukhov length

$$L = \frac{u^{*2}}{k(g/T)(\theta^* + 0.61q^*T)} \quad (9)$$

g is the acceleration of gravity, and T is a reference temperature assumed to be the air temperature near the surface. When the Φ functions have been specified from the literature [Brutsaert, 1982; Morris, 1989], equations (3)-(5) can be integrated to give equations which relate fluxes to differences in wind speed, temperature, and specific humidity between two levels z_1 and z_2 (30 and 180 cm, depending on the snow height).

$$u^* = k(u_2 - u_1) [\ln(z_2/z_1) - \Psi_m(z_2/L) + \Psi_m(z_1/L)]^{-1} \quad (10)$$

$$\theta^* = k(\theta_2 - \theta_1) [\ln(z_2/z_1) - \Psi_h(z_2/L) + \Psi_h(z_1/L)]^{-1} \quad (11)$$

$$q^* = k(q_2 - q_1) [\ln(z_2/z_1) - \Psi_v(z_2/L) + \Psi_v(z_1/L)]^{-1} \quad (12)$$

The Ψ functions Ψ_m for momentum, Ψ_h for heat, and Ψ_v for water vapor are the vertically integrated forms of the Φ functions, and they depend on the stability of the surface layer:

Unstable conditions ($z/L < 0$)

$$\Psi_m = 2 \ln \left[\frac{1+x}{2} \right] + \ln \left[\frac{1+x^2}{2} \right] - 2 \arctan(x) + \frac{\pi}{2} \quad (13)$$

$$\Psi_h = \Psi_v = 2 \ln \left[\frac{1+x^2}{2} \right]$$

with $x = (1 - 16 z/L)^{1/4}$

Stable conditions ($0 < z/L < 1$)

$$\Psi_m = \Psi_h = \Psi_v = -5 z/L \quad (14)$$

Very stable conditions ($z/L > 1$)

$$\Psi_m = \Psi_h = \Psi_v = -5 [\ln(z/L) + 1] \quad (15)$$

The calculations were performed iteratively: the first estimates of u^* , θ^* , and q^* were obtained from equations (10)-(12), assuming first that $z/L = 0$ (logarithmic profiles) and the results were used to calculate L from equation (9). According to the sign of L , this value of L could be substituted back into equations (10)-(12) to

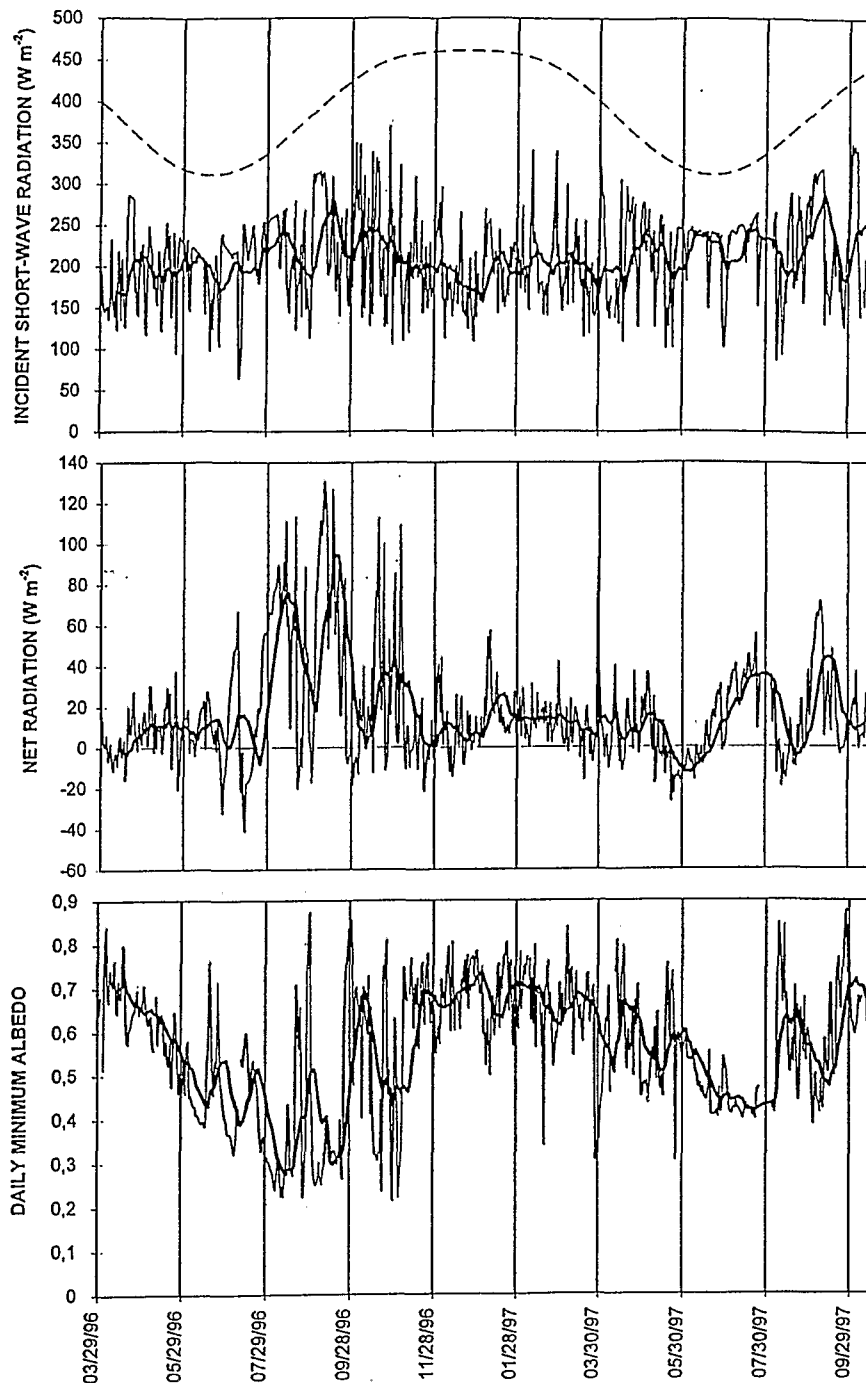


Figure 4. Variation in the daily mean values of incident short-wave radiation, net all-wave radiation, and in the daily minimum of albedo over the entire measuring period from March 29, 1996 to October 15, 1997, measured at 5150 m asl. The thick line is the 15-day running mean. The dashed line is the extraterrestrial irradiance.

improve the estimates of u^* , θ^* , and q^* . The scheme usually converged within four iterations giving values of H and LE from equations (7)-(8).

4.2.2. Surface warm layer. In the Monin-Obukhov theory the fluxes of momentum, sensible, and latent heats are supposed to be constant with height. Therefore, turbulent fluxes calculated between z_1 and z_2 are equal to surface turbulent fluxes. This assumption gives a great power to the Monin-Obukhov theory because surface conditions (roughness, temperature) are not necessary to be investigated to get surface fluxes. The portion of

the atmosphere to which this condition applies is referred to as the "constant flux layer" [Male and Granger, 1981]. Nevertheless, over a melting snow surface, De la Casinière [1974], Halberstam and Schiedge [1981], and more recently, Meesters *et al.* [1997] have reported temperature profile anomalies within the first meter of atmosphere probably due to the radiative heating of the air above the snow surface, leading to fluxes variable with height. On Zongo Glacier, a similar situation is observed: during the day a highly stable sublayer forms near the surface, with a persistent warm layer around 20-30 cm, whereas at night, profiles agree



Figure 5. Forty centimeter high penitents at the glacier surface at 5150 m asl (August 4, 1997). The scale is given by the 45 cm long ice axe.

more with classical loglinear forms found in stable air. Figure 6 shows the vertical gradient of air temperature between 30 and 180 cm above the glacier surface at the weather station, for whatever period of 10 days (September 1-10, 1997, in Figure 6). During the day this gradient is negative, although the temperature at 30 cm is positive which suggests that there is a warm layer around 30 cm. By night this gradient is positive, and representative of a highly stable surface boundary layer. Although many authors are still doubtful concerning this warm layer and prefer to invoke measurement deviation due to radiational errors, the strong and systematic perturbation of the observed temperature profiles over Zongo Glacier cannot be related to sensor inaccuracy and then acts as a proof for the actual existence of this layer.

On Zongo Glacier, at night, while the constant flux layer was well developed over the surface, turbulent fluxes were estimated by using the Monin-Obukhov method described above, but during the day, as soon as the warm layer appeared, the fluxes were estimated using the Monin-Obukhov method between the surface and the first measurement level z_1 ($z_1 = 30$ cm, depending on the snow height). During the day, snow was melting at the field site, and thus the surface temperature was assumed to be 0°C , and the

vapor pressure was supposed to be the saturation vapor pressure (6.1 hPa). Applying the Monin-Obukhov method between the surface and z_1 consists actually in using the bulk aerodynamic approach with stability correction. Since surface temperature measurements were lacking at night, it was not possible to apply the bulk aerodynamic method as soon as the surface temperature was below the melting point. Over small glaciers a katabatic layer often exists close to the surface and the wind profile exhibits a low-level wind maximum [e.g., Martin, 1975]. On Zongo Glacier, since u_1 is always lower than u_2 , this phenomenon does not seem to occur, and the Monin-Obukhov theory can be applied.

4.2.3. Roughness lengths. Since during the day the Monin-Obukhov similarity theory must be applied between the surface and z_1 , surface roughness parameters for momentum z_{0m} , for temperature z_{0T} , and for humidity z_{0q} must be evaluated. By definition, z_{0m} is the height where the horizontal component of the wind speed is zero, $u(z_{0m}) = 0$. The roughness lengths depend mainly on surface geometry but also on wind speed for z_{0m} [Plüss, 1997] or on the absorption of short-wave radiation for z_{0T} [Meesters *et al.*, 1997]. In neutral conditions, z_{0m} is derived from the following equation

Table 3. Annual Mean Discharges in L s^{-1} of 4 Hydrological Years With Their Respective Means of Wet and Dry Seasons

	Sept. 93 - Aug. 94	Sept. 94 - Aug. 95	Sept. 95 - Aug. 96	Sept. 96 - Aug. 97
Period	EY,WS,DS	EY,WS,DS	EY,WS,DS	EY,WS,DS
Mean discharge	130,234,78	160,246,88	169,247,67	122,173,62

EY stands for entire year, WS for wet season (November-March), DS for dry season (May-August).

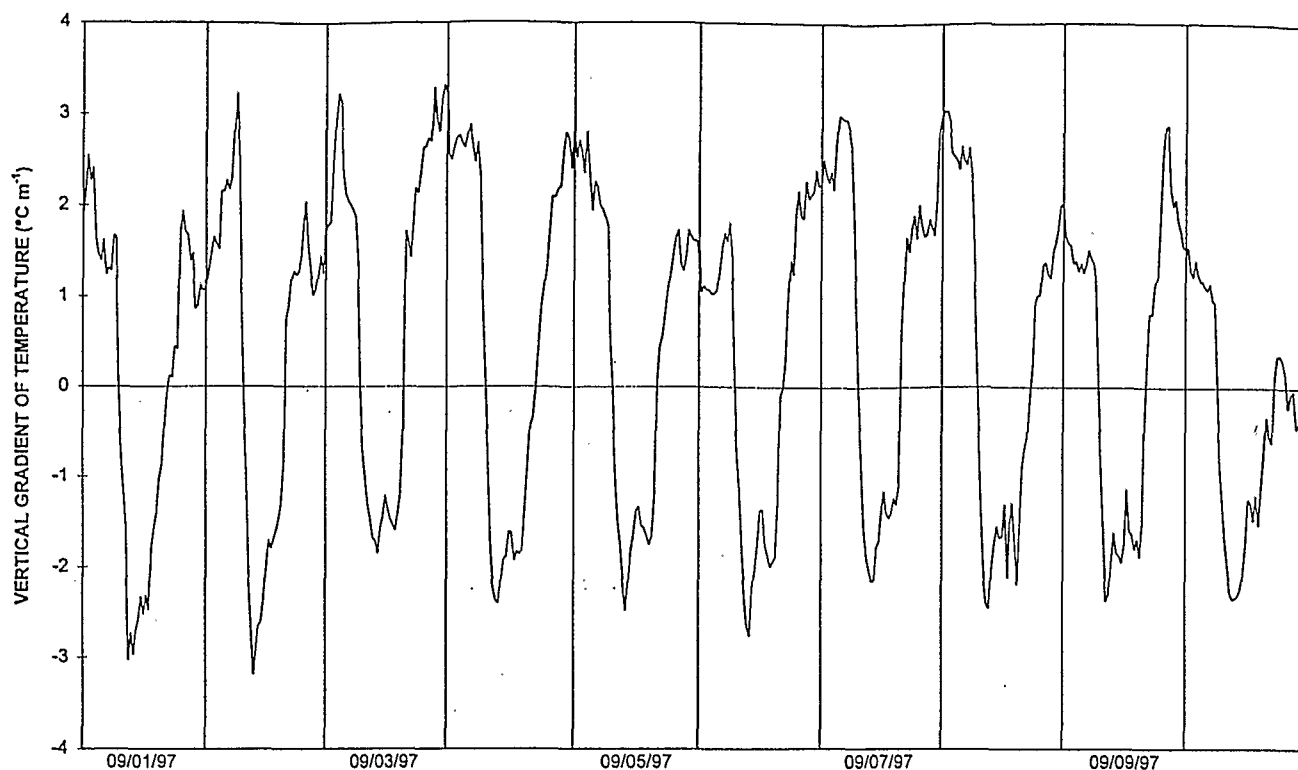


Figure 6. Vertical gradient of air temperature between 30 and 180 cm above the glacier surface at 5150 m asl, for the period September 1-10, 1997. Gradients are positive at night and negative during the day, while a warm layer develops around 30 cm.

$$z_{0m} = \frac{(u_2 \ln z_1 - u_1 \ln z_2)}{(u_2 - u_1)} \quad (16)$$

Therefore z_{0m} can be evaluated from selected wind profiles corresponding to near neutral conditions ($z/L < 0.01$). However, the scatter is too large to calculate an average. The same problem is observed with z_{0T} and z_{0k} . This problem is of great importance because the energy balance is extremely sensitive to the choice of surface roughness [Hock and Holmgren, 1996]. For this reason, although many authors suggested that z_{0T} and z_{0k} are 1 or 2 orders of magnitude lower than z_{0m} [e.g., Ambach, 1986; Andreas, 1986; Morris, 1989; Hock and Holmgren, 1996; Meesters et al., 1997], the three roughness lengths were set equal to each other: $z_{0m} = z_{0T} = z_{0k} = z_0$. This assumption is probably correct for smooth surfaces, but over rough surfaces, this may induce an overestimation of the turbulent fluxes [Bintanja and Van den Broeke, 1995]. The value of z_0 is estimated iteratively in order to have the best agreement between calculated latent heat flux and daily sublimation as measured by lysimeters on the field site. This indirect method to obtain z_0 based on direct field measurements is not suitable to distinguish z_{0m} from z_{0T} and z_{0k} because as many triplets of values as we want might fit the direct measurements. Therefore keeping a unique value is more logical even if it may not be the truth. The value of z_0 obtained by this method is therefore a kind of bulk parameter but has the dimension of a roughness length since it is a compilation of the three roughness parameters. For this reason, z_0 is probably not so different from z_{0m} , at least for smooth surfaces. From season to season, the "bulk roughness parameter" z_0 at the weather station changes a lot, going from a minimum value of 2×10^{-3} m on smooth surfaces and recent snow during the wet season to a maximum value of 3×10^{-2}

m corresponding to rough surfaces of 40 cm high penitents typical of the middle of the dry season. Table 4 gives the values of z_0 along the entire measuring period. In total, 24 representative days of the dry and the wet seasons had direct sublimation measurements good enough to adjust the values of z_0 . The rest of the time, the values of z_0 were attributed by comparing photographs taken every 10 days while checking the weather station to photographs of the glacier surface the days when lysimeter measurements had been performed.

4.2.4. Accuracy. The accuracy of this method in calculating the turbulent fluxes is very difficult to estimate. Indeed, we have seen in this section that this method is based on the assumption that turbulent fluxes are constant with height within the boundary

Table 4. Values of z_0 for Entire Measuring Period

Period	z_0 , mm
March 29 to April 30, 1996	2
May 1-31, 1996	10
June 1 to July 31, 1996	30
Aug. 1-31, 1996	20
Sept. 1-30, 1996	10
Oct. 1-31, 1996	4
Nov. 1, 1996 to April 30, 1997	2
May 1-31, 1997	5
June 1-15, 1997	10
June 16-30, 1997	20
July 1 to Aug. 6, 1997	30
Aug. 7-21, 1997	20
Aug. 22 to Sept. 15, 1997	10
Sept. 16 to Oct. 15, 1997	4

surface layer. However, the warm layer leads to a strong thinning of the constant flux layer by day which might be reduced to 20 or 30 cm thick; although at night, the boundary surface layer shows a more typical thickness of several meters. In this context the chance that the lower sensor is exactly located at the temperature maximum is very weak, which means that gradients used to calculate turbulent fluxes may slightly differ from natural gradients. This difference cannot be evaluated precisely. Nevertheless, since calculated latent heat flux values are calibrated on direct sublimation measurements thanks to the "bulk roughness parameter" z_0 , qualitative and quantitative results must be trustworthy, and a reasonable accuracy is believed.

4.3. Conductive Energy Flux in Snow/Ice

The conductive heat transfer within the snowpack or the ice tends to be small when compared to radiative or turbulent fluxes [Marks and Dozier, 1992]. Therefore it can be greatly simplified. The heat flux into the snow/ice is estimated from temperature-depth profiles of 7 Cu-Cst thermocouples down to a depth of 2.7 m, depending on the snow height. This heat flux is given by [Oke, 1987]

$$G = -K \frac{\partial T}{\partial z} \quad (17)$$

where K is the thermal conductivity of snow/ice (in $W m^{-1} K^{-1}$), T is the snow/ice temperature, and z is the depth. Below 50 cm, temperature sensors did not show any daily variation, and the local gradient of temperature is replaced by the finite difference between -50 cm and the surface. Since this flux is of minor importance compared to the others, a coarse estimate of T_s is sufficient (logarithmic extrapolation of air temperatures with an upper limit of 0°C). K is not a simple constant for a given soil but varies both with depth and with time. Bulk averages of K depend upon the conductivity of the soil particles, the soil porosity and the soil moisture content. K is greater for ice ($K_{\text{pure ice, 0°C}} = 2.24 W m^{-1} K^{-1}$) than for old snow ($K_{\text{old snow}} = 0.42 W m^{-1} K^{-1}$) [Oke, 1987]. According to the state of the upper layers at the weather station (ice or snow) the values of K are varying between a minimum value of 0.4 and a maximum of $1.8 W m^{-1} K^{-1}$. While the 50 cm thick surface layer was composed of both snow and ice, a weighted average was assumed for K .

4.4. Energy Balance of Snowpack

Changes in the internal energy of the snowpack ($\Delta Q_M + \Delta Q_S$) are calculated as a residual using equation (1). If the left-hand side of the equation (1) is positive, energy is available for the snow/ice; it will be used first to increase the snow/ice temperature until its upper limit 0°C ($\Delta Q_S > 0$ and $\Delta Q_M = 0$), and then when the surface temperature is 0°C, melting occurs ($\Delta Q_M > 0$). Otherwise, if it is negative, the reverse situation is observed: the meltwater of the snowpack refreezes ($\Delta Q_M < 0$), and afterward, snow/ice temperature decreases ($\Delta Q_S < 0$). ΔQ_S is the rate of gain/loss of heat of a vertical column extending from the surface to the depth z at which seasonal variations in temperature are negligible (about 0.5 m on Zongo Glacier) [Lliboutry, 1964; Paterson, 1994].

$$\Delta Q_S = \int_0^z \rho_i c_i (\partial T_i / \partial t) dz \quad (18)$$

Here ρ_i is the snow/ice density, c_i is the snow/ice specific heat capacity ($\approx 2090 J K^{-1} kg^{-1}$), T_i is the snow/ice temperature, and t is time. Conduction is not the only means of heat transfer. Refreezing of surface meltwater that percolates through the

snowpack, short-wave radiation penetration or air and vapor circulation can also transfer heat within the snowpack [Paterson, 1994]. ΔQ_S can be derived from Cu-Cst thermocouples which give the snow/ice temperature as halfhourly means at various depths. Nevertheless, we notice that vertical profiles of temperature within the snowpack show most of the time a daily cyclic pattern whatever the season: during typical days, around noon, the snowpack returns to an isothermal situation with temperatures close to the melting point. Therefore considering daily means, ΔQ_S usually remains zero because the gain of heat during the day is compensated by the loss of heat at night. This situation is typical for every snowcover or every glacier under melting conditions, which are encountered throughout the year on Zongo Glacier. Therefore looking at daily means, the change of the internal energy of the snowpack is reduced to the latent heat storage change due to melting or freezing. ΔQ_M is converted to mass units using the latent heat of fusion L_f ($L_f = 3.34 \cdot 10^6 J kg^{-1}$)

$$\Delta Q_M = L_f \dot{M} \quad (19)$$

with \dot{M} the meltrate in mass per unit area per unit time ($kg m^{-2} s^{-1}$ or $mm s^{-1}$). Thus equation (1) lets calculate daily values of \dot{M} (in $mm d^{-1}$). Moreover, \dot{M} has been measured directly on the field site with the "fusion-box," during selected periods. Table 5 presents the comparison between the daily melting \dot{M} measured by the fusionbox and obtained as a residual of equation (1). There is a fairly good agreement between measurements and calculations which proves that this energy balance is accurate enough to relate it to daily fusion at the glacier surface. For a few days, there is a discrepancy between measurements and calculations due to various reasons. On November 15 and 16, 1996, numerous snowfalls have affected the collection of meteorological data at the automatic weather station (upper dome of the net radiometer sometimes covered by falling snow which leads to an underestimation of net all-wave radiation), and thus the calculated \dot{M} is too low. On August 4, 1997, we observed edge effects on the fusionbox which led to an artificially exaggerated melting. In conclusion, the discrepancies observed might be due to the fusion-box measurement inaccuracy (capillarity retention or edge effects) or to meteorological data inaccuracy under very snowy conditions.

Table 5. Values of the Daily Melting \dot{M} measured With the Fusion Box and Calculated From the Energy Balance Equation for Some Selected Days While on the Field Site

Date	Measured \dot{M} , $mm d^{-1}$	Calculated \dot{M} , $mm d^{-1}$
Aug. 23, 1996	1.2	0
Aug. 24, 1996	8.2	8.06
Aug. 25, 1996	16.1	17.63
Aug. 26, 1996	7.6	9.34
Nov. 14, 1996	4.3	3.58
Nov. 15 and 16, 1996	4.5	0.30
Nov. 17, 1996	3.7	2.65
March 3, 1997	0.7	1.18
March 4, 1997	1.7	0
March 5, 1997	1.2	0
March 7, 1997	0	0
May 19-27, 1997	0	0
Aug. 4, 1997	5.3	0
Aug. 5, 1997	7.6	6.64
Aug. 7-14, 1997	0	0

Nevertheless, such conditions are very scarce, and therefore qualitative and quantitative results of this energy balance study are believed to be representative.

5. Results

5.1. Energy Balance Results

The monthly mean energy balance terms for the entire measuring period are shown in Figure 7. A number of interesting features can be noted. The net all-wave radiation is the main source of energy at the glacier surface but is highly variable from month to month and from year to year. Indeed, the net all-wave radiation is a function of albedo, and according to the firnline altitude, the albedo at the weather station (Figure 4) may vary rapidly from 0.7 (when a snow cover is still present) to 0.3 (on bare dirty ice). Thus for the same month, net all-wave radiation may change significantly from one year to another. Here, for example, there is 1 order of magnitude difference between the monthly mean net radiation of August 1996 ($R = 53 \text{ W m}^{-2}$, $\alpha_{\text{min}} = 0.4$) and August 1997 ($R = 5 \text{ W m}^{-2}$, $\alpha_{\text{min}} = 0.6$). The second most important surface energy flux is the latent heat flux. LE is negative throughout the year, indicating that the ice surface loses mass by sublimation. For the hydrological year September 1996 to August 1997 the ablation due to sublimation is as high as 200 mm, which corresponds to an annual mean value of 0.54 mm d^{-1} ($LE = -18 \text{ W m}^{-2}$). Table 6 lists annual mean values of the energy balance fluxes and mean values for both seasons. One peculiarity is that most of this sublimation occurs during the dry season with a mean rate of 0.94 mm d^{-1} (May–August 1997) and is very reduced during the wet season with a mean rate of 0.22 mm d^{-1} (November 1996 to February 1997). The latent heat flux is then the main heat sink of this energy budget and is highly variable

with the seasons, showing high sublimation rates during the dry season. The sensible heat flux is positive throughout the year, which suggests that the surface boundary layer is almost always in stable conditions. H is nonnegligible but remains small with slightly lower values during the wet season (mean value of 4.4 W m^{-2} between November 1996 and February 1997) and higher values during the dry season (9.1 W m^{-2} between May and August 1997). G is also positive throughout the year. It remains extremely small during the wet season, but during the dry season, because of slightly lower temperatures, it is higher with a mean value of 4.1 W m^{-2} .

Figures 4 and 8 show the temporal variation in the daily mean values of the energy balance components. The highly variable wind speed, air temperature, and specific humidity on a timescale of a few days cause strong fluctuations in H and LE , especially during the dry season. LE is very dependent on the hour of the day at which the wet air masses advected from the lowlands arrive at the field site. Indeed, in the morning, as soon as the Sun rises, the atmosphere is dry and LE is high. When wet air masses invade the glacier, the relative humidity arises rapidly and LE drops. From one day to another, these air masses, coming from the eastern lowlands, might invade the glacier sooner or later in the afternoon, or even might not invade it, which leads to strong fluctuations of daily values of LE on the timescale of a day. Net all-wave radiation also shows strong fluctuations on the timescale of a few days (Figure 4) in relation to the highly variable albedo, as already discussed in section 3. Therefore since net all-wave radiation is the main source of energy at the glacier surface, albedo is the principal factor controlling the energy balance on Zongo Glacier.

The mean daily cycle of the energy balance terms and of air temperature, wind speed, and relative humidity for the wet and dry seasons of the hydrological year 1996–1997 is shown in Figure 9.

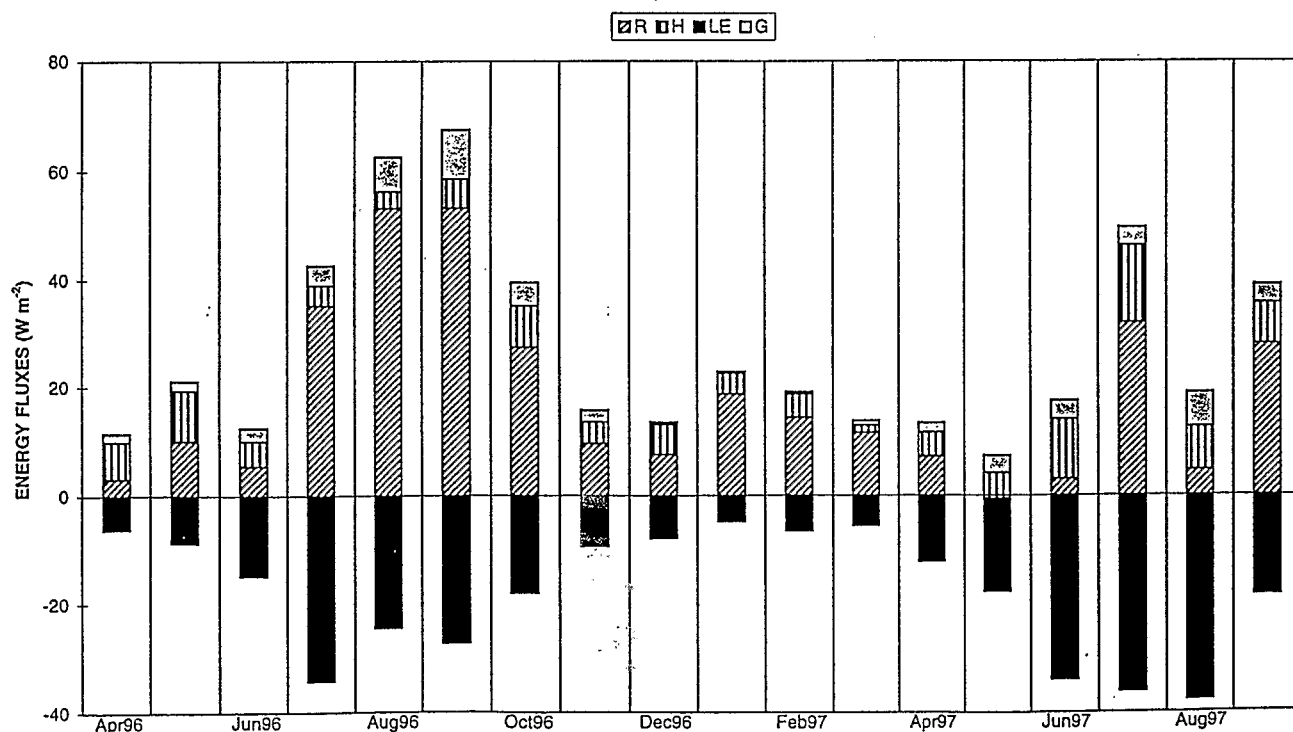


Figure 7. Monthly mean values of each component of the energy balance over the entire measuring period (April 1996 to September 1997) at 5150 m asl. R is the net all-wave radiation, LE is the latent heat flux, H is the sensible heat flux, and G is the conductive heat flux. A positive flux indicates a flow of energy toward the surface.

Table 6. Mean Values Over Entire Measuring Period, Over Hydrological Year 1996-97, and Over Wet and Dry Seasons of Energy Flux Components

Variable, $W m^{-2}$	Entire Period, 521 days	Sept. 96 to Aug. 97	Wet Season Nov. 96-Feb. 97	Dry Season May-Aug. 97
R	16.9	16.5	12.7	10.5
LE	-17.0	-17.7	-7.3	-30.9
H	6.0	6.0	4.4	9.1
G	3.0	2.8	0.8	4.1
ΔQ_M	8.9	7.2	10.6	-7.2

R is the net all-wave radiation, LE is the latent heat flux, H is the sensible heat flux, G is the conductive heat flux, and ΔQ_M is the melting component.

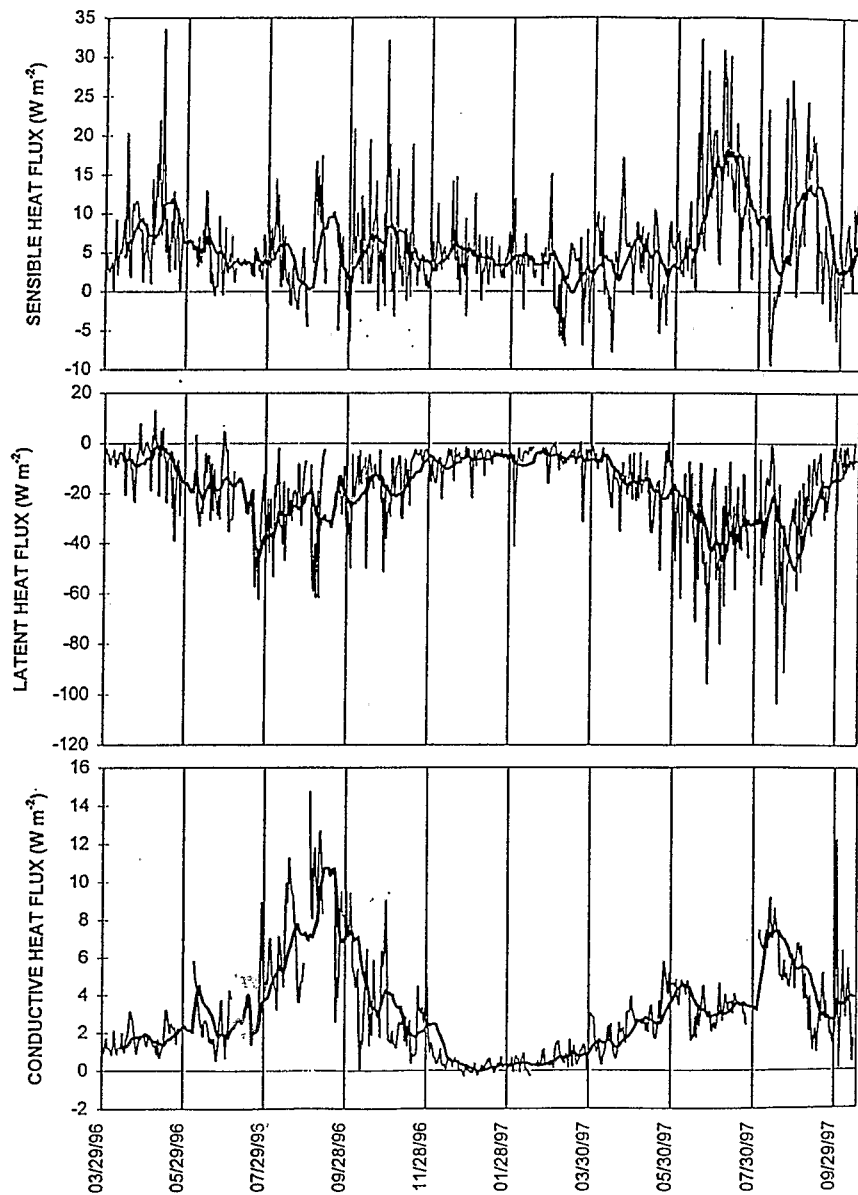


Figure 8. Daily mean values for sensible heat flux (H), latent heat flux (LE), and conductive heat flux (G) over the entire measuring period (March 29, 1996 to October 15, 1997). Note that the graphs have different vertical scales. The thick line is the 15-day running mean.

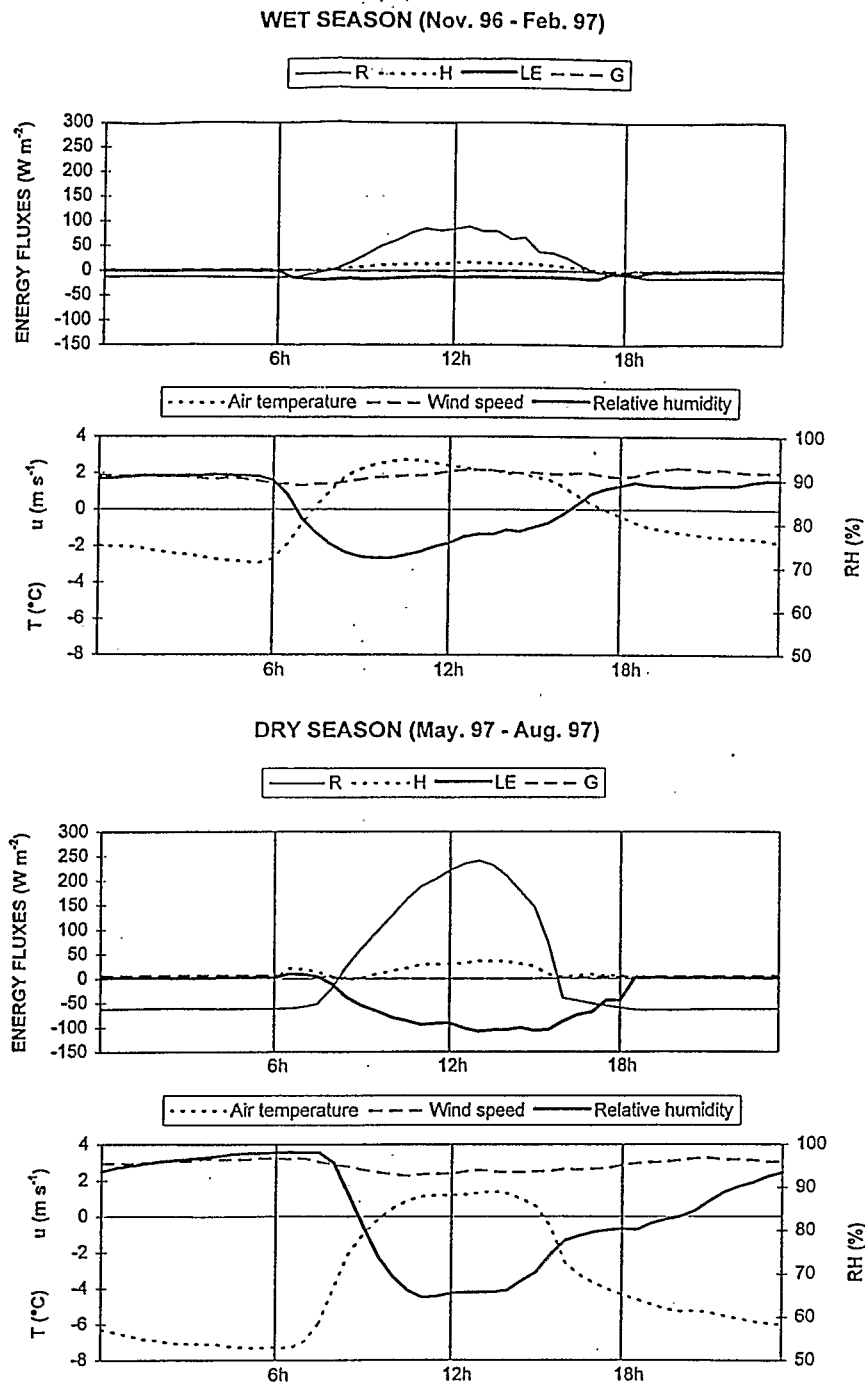


Figure 9. Mean daily cycle of the different energy balance terms and various meteorological quantities (air temperature, wind speed, and relative humidity) over the wet and dry seasons.

For both seasons, net all-wave radiation is negative at night (radiative cooling of the surface) and positive during the day. Because of a reduced cloudiness during the dry season, the radiative cooling of the surface is higher than during the wet season where net all-wave radiation is less negative. During the day a larger part of incident solar radiation is reflected by clouds during the wet season than during the dry season, resulting in a reduced net all-wave radiation. The shading by mountains surrounding the field site at the end of the afternoon is responsible for the asymmetrical shape of the daily cycle of R , especially during the dry season. The turbulent fluxes present a similar mean daily cycle for both seasons: at night, the boundary surface layer is

very stably stratified ($z/L > 1$), and thus turbulent fluxes are negligible and during the day, the stratification of the lower atmosphere remains moderately stable ($0 < z/L < 1$), with positive values for H and negative values for LE . Unstable conditions ($z/L < 0$) are sometimes encountered in the early morning (around 0800-0900 LT) while snow/ice surface is heated by incident short-wave radiation and air temperature is still negative. In these cases rather typical of the dry season, H is negative. After a while, the temperature at the surface reaches its upper limit $0^{\circ}C$, air temperature keeps increasing to positive values and then the lower atmosphere becomes moderately stable with a positive sensible heat flux. The main difference between the two seasons comes

from the latent heat flux which is very high during the dry season because of the higher wind speed and stronger gradients of vapor pressure between the surface and the first measurement level than during the wet season. Indeed, the average daily cycle in relative humidity (Figure 9) shows that the humidity in daytime in the dry season is lower than in the humid season, which leads to higher vertical gradients of humidity. Moreover, the large annual cycle of the bulk roughness parameter z_0 (Table 4), which describes the seasonal variability of the roughness of the glacier surface, contributes greatly to explain the seasonality of the turbulent fluxes. The conductive energy flux in the snow/ice is nil in daytime and positive at night with slightly higher values during the dry season. Indeed, during this season the radiative cooling of the surface is increased by the absence of cloudiness, and therefore surface temperature can reach its minimum values, the temperature gradient within the snowpack is increased which leads to higher values for G .

5.2. Energy Balance and Mass Balance

Knowing the monthly accumulation c given by the monthly precipitation recorded by storage rain gages located around the glacier on the moraine [Francou *et al.*, 1995] and the monthly local mass balance b obtained from stake measurements or ultrasound sensor records, it is possible to get the monthly ablation ($a = b - c$) at the field site. The c is measured directly in millimeters of water in the rain gages, but b must be turned in millimeters water equivalent (mm w. e.) using mean values for snow/ice density. On the other hand, the monthly ablation (because of melting and sublimation ($a = m + s$)) can also be calculated from the energy balance study. Figure 10 compares the measured and calculated monthly ablation in the vicinity of the weather station, at 5150 m asl, and Table 7 lists the mean values of these two variables for the entire measuring period, for the hydrological year 1996-1997, as well as for the wet and dry seasons. There is a fairly good agreement between the two

variables with a correlation coefficient r^2 of 0.85 for 18 months. The observed discrepancies might be explained by some inaccuracies in the snow/ice density estimates or in the used accumulation values. Indeed, precipitation is recorded on the moraine about 400 m away from the meteorological station, whereas it is well known that the spatial variability of accumulation is very high, as shown by Vincent *et al.* [1997] on an Alpine site. Therefore the precipitation recorded on the moraine might differ slightly from the local accumulation at the field site, which leads to some errors for the measured ablation at the field site, especially during the wet season. Indeed, note that this discrepancy is higher during the wet season than during the dry season (Table 7).

6. Discussion

6.1. Typical Features of Energy Balance of Outer Tropics' Glaciers

The glaciers of the outer tropics are subject to peculiar climatic conditions which induce the following specifications concerning their energy balance:

1. Net all-wave radiation is the main source of energy at the glacier surface and does not show any well-marked seasonality along the year.
2. Latent heat flux is negative throughout the year, indicating a mass loss by sublimation: sublimation is high during the dry season and very reduced the rest of the year.
3. Sensible heat flux remains continuously positive along the year, as suggested by Kaser *et al.* [1996], for Yanamarey Glacier (Cordillera Blanca, Peru) and is of minor importance compared to the previous fluxes.
4. The conductive heat flux in the snow/ice remains extremely small during the humid season but is responsible for a nonnegligible upward energy flux during the dry season.

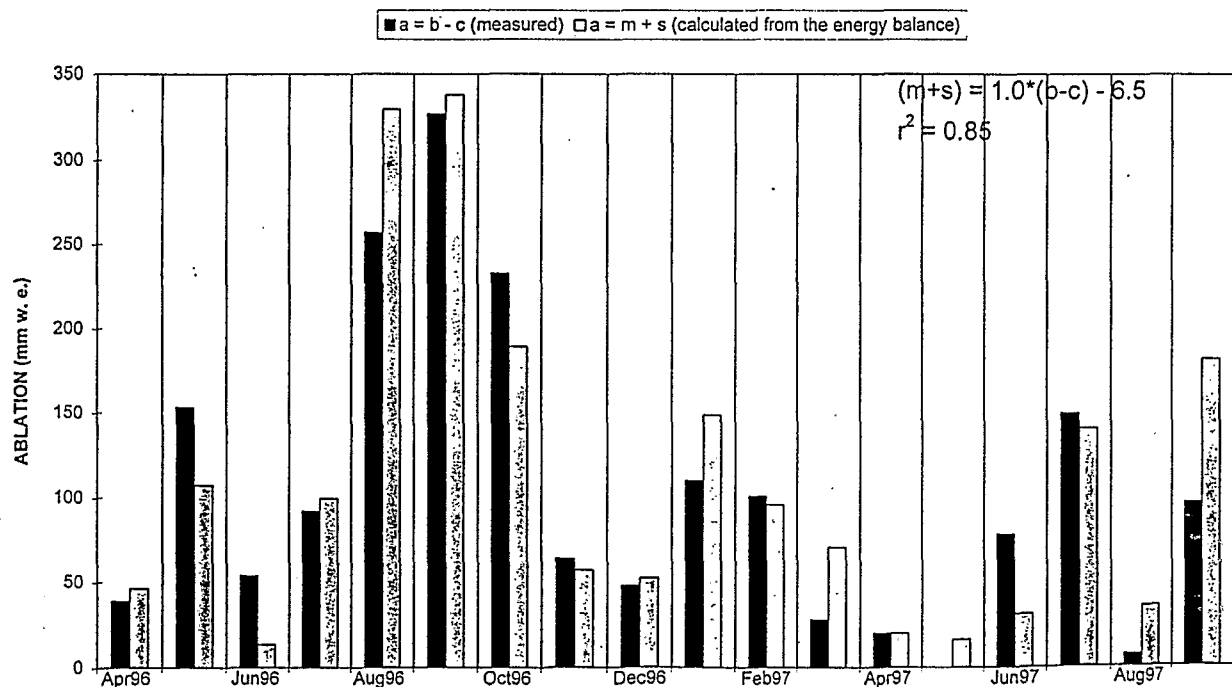


Figure 10. Monthly ablation at 5150 m asl measured with stakes and rain gages ($a = b - c$, mass balance minus accumulation) and calculated from the energy balance equation ($a = m + s$, melting plus sublimation).

Table 7. Values of Local Ablation (mm w. c.) at 5150 m asl Over Entire Measuring Period, Over Hydrological Year 1996-97, and Over Wet and Dry Seasons Measured With Stakes and Rain gages (a = b-c, Mass Balance Minus Accumulation) and Calculated From the Energy Balance Equation (a = m+s, Melting Plus Sublimation)

Variable, mm w. c.	Entire Period, 521 days	Sept. 96 to Aug. 97	Wet Season Nov. 96 to Feb. 97	Dry Season May-Aug. 97
b	-495	-36	+327	-165
c	1343	1110	630	70
b - c	-1838	-1146	-303	-235
m	-1673	-994	-327	-107
s	-303	-202	-27	-117
m + s	-1976	-1196	-354	-224

6.2. Energy Balance, Mass Balance, and Runoff Seasonality

Neither net all-wave radiation, nor sensible heat flux is variable enough with the seasons to explain the large seasonality of the proglacial stream discharge shown in section 3 (Figure 2 and Table 3). On the other hand, the contribution of latent heat flux to the energy balance is very variable (Figures 7 and 9) and is responsible for this runoff seasonality, as already discussed by Wagnon *et al.* [1998]. During the dry season, at the glacier surface, the energy input as net all-wave radiation, sensible heat, flux and conductive heat flux in the snow/ice is almost entirely consumed by the high sublimation (penitents grow rapidly at the surface), and therefore melting is reduced and discharge is low. Whereas during the wet season, the lower gradients of humidity of the boundary surface layer stops the sublimation, and the energy input is used for melting, which leads to high discharge. In conclusion, in the outer tropics, humidity is an important meteorological input controlling the seasonality of the glacier mass balance and the proglacial stream runoff, because it is responsible for the sharing of the energy available at the surface between two sinks, sublimation or melting.

This is an important peculiarity of the glaciers of the outer tropics whose mass balance is ruled by sublimation and therefore by humidity, whereas under midlatitude or polar conditions, the latent heat flux is most of the time considered as negligible [e.g., Male and Granger, 1981; Plüss and Mazzoni, 1994; Hock and Holmgren, 1996]. Quantitatively, sublimation still represents only a minor part of the total local ablation at the field site: 202 mm over an annual total of 1196 mm for the hydrological year 1996-1997, that is to say, less than 17%. However, if comparing the amount of energy consumed by sublimation $L_s E$ to the one consumed by melting $L_f M$ for this hydrological year 1996-1997 (respectively $572.5 \times 10^6 \text{ J m}^{-2}$ and $332.0 \times 10^6 \text{ J m}^{-2}$), sublimation is responsible for more than 63% of the available energy consumption. In this context, tropical glaciers are very sensitive to specific humidity changes due to the "greenhouse effect" for instance. Indeed, Hense *et al.* [1988] have reported that a change of the greenhouse effect is responsible not only for a warming but also for a specific humidity increase of 0.6 g kg^{-1} in the 500-700 hPa level in the equatorial belt between 1965 and 1984. A specific humidity increase reduces the latent heat flux which saves energy for melting: for example, if other fluxes are assumed to remain constant, a 10% decrease of the latent heat flux during the hydrological year 1996-1997 will lead to a 17% increase of the

melting and a 13% increase of the total ablation. However, this greenhouse forcing leads also to sensible heat flux and net long-wave radiation increase, as reported by Hastenrath and Kruss [1992] on Mount Kenya, which explains the dramatic retreat of tropical glaciers since 1980. In conclusion, tropical glaciers are likely to be some climatic indicators very sensitive to climatic changes like the greenhouse effect.

Figure 11 compares the monthly melting at 5150 m asl derived from the energy balance equation (1) to the monthly mean discharge of the proglacial stream. As Zongo Glacier is small and as the timescale is one month, no long-term storage of the meltwater originating at 5150 m asl, inside the glacier, is taken into account, and therefore the local melting at 5150 m asl might be compared to the proglacial stream discharge. The amount of snow/ice lost by melting at 5150 m asl on Zongo Glacier is highly variable from month to month but does not have any well-marked seasonality. It even tends to have an opposed variability to the proglacial stream discharge, showing a reduced melting during the wet season although the proglacial stream discharge is the highest. This opposition shows that during the humid season, the weather station is located in the accumulation area, outside the area where strong ablation conditions occur. However, the rest of the time, the melting calculated at 5150 m asl agrees fairly well with the discharge recorded at the limnometric station which suggests that the equilibrium line is higher in altitude. This observation is confirmed while plotting the mass balance measured by the different ablation stakes as a function of altitude, first for the wet season (September 1996 to February 1997) and second for the dry season (March - August 1997) (Figure 12): the vertical budget gradient db/dz is much higher during the wet season than during the dry one. There is here a paradox because high discharges observed during the wet season are caused by very strong melting conditions prevailing on a considerably reduced ablation area, whereas lower discharges the rest of the year come from weak melting conditions occurring on a much larger ablation area. These strong melting conditions of the wet season in the lower part of the glacier are explained first by the low albedo (bare ice surfaces covered by impurities) and second by the negligible latent heat flux, which saves energy for melting. In order to get a better insight into the functioning of Zongo Glacier, it would have been preferable to set the weather station lower in altitude around 5000 m asl but the very strong ablation at this altitude would have been a problem in the monitoring of the meteorological station. In conclusion, albedo and humidity are the two main factors governing the glacier energy and mass balance and proglacial stream runoff. Therefore if for one reason the wet season is poor in precipitation, like for the El Niño Southern Oscillation (ENSO) event of 1991-1992 [Francou *et al.*, 1995], the snow cover at the glacier surface is thinner and thus disappears more rapidly, the area of low albedo becomes larger, and therefore the ablation area characterized by very strong melting conditions is larger. Thus melting is very high, proglacial stream discharge is maximum within 1 or 2 months, and the glacier annual mass balance is strongly negative, like for the ENSO year 1991-1992. This functioning of Zongo Glacier is different compared to midlatitude or polar glaciers.

7. Summary and Conclusions

Within the tropical half of Earth, the Zongo Glacier of Cordillera Real, Bolivia, is the only place where an energy balance monitoring program has been sustained for more than 1 year. This glacier belongs to the outer tropics characterized by the lack of

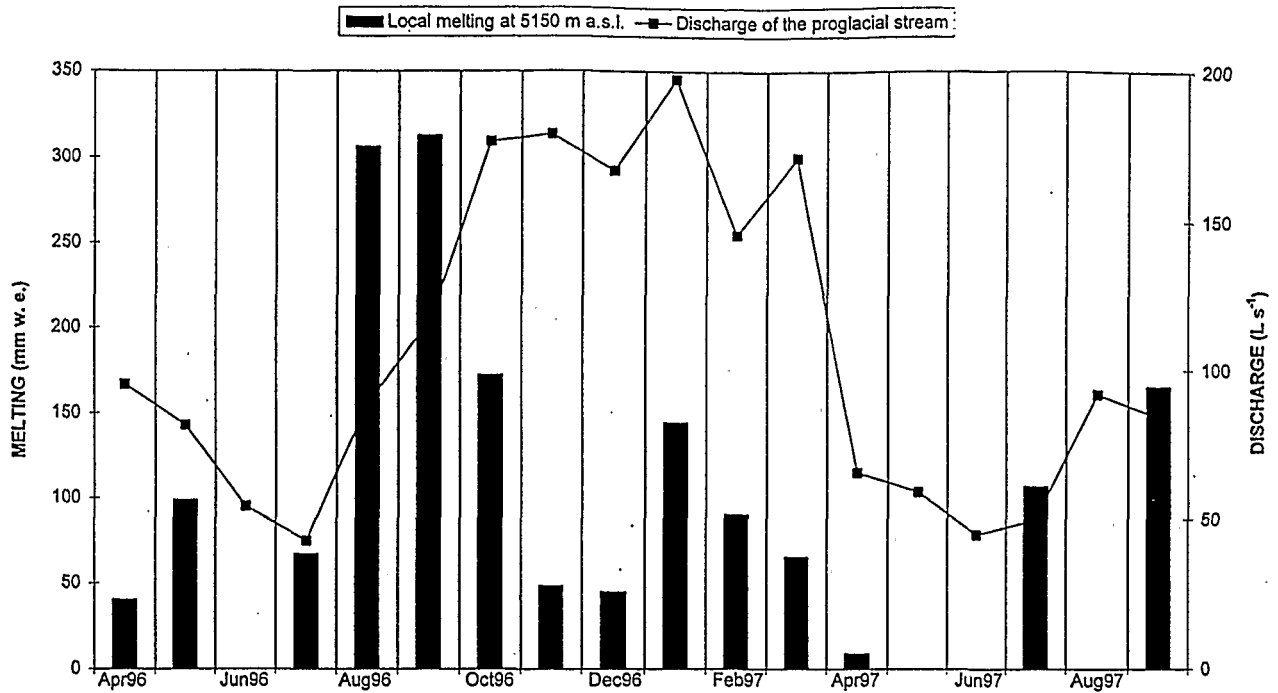


Figure 11. Monthly melting at 5150 m asl calculated from the energy balance equation and monthly mean discharge recorded at the limnometric station at 4830 m asl.

any appreciable thermal seasonality and a hydrological year punctuated by one dry and one wet season. Since March 1996, an automatic weather station has been recording all the meteorological data (net all-wave radiation, incident and reflected short-wave radiation, wind speed and direction, aspirated air temperature, vapor pressure, snow/ice temperatures, every day ablation) needed to compute the local energy balance and to compare it to the local mass balance. The Monin-Obukhov similitude theory has been used to calculate the turbulent fluxes over the surface. The roughness parameters for momentum, temperature, and humidity were all chosen equal to each other and were derived from direct sublimation measurements performed regularly on the field site. The value z_0 is therefore a bulk parameter used to calibrate the calculated latent heat flux; z_0 depends mainly on the surface geometry and is then very variable

from month to month, going from a minimum value of 2×10^{-3} m for smooth surfaces covered by fresh snow (wet season) to a maximum value of 30×10^{-3} m corresponding to 40 cm high penitents at the surface (dry season). Above melting snow surfaces, we noticed the presence of a warm layer 20-30 cm above the surface.

Concerning the annual mean budget (hydrological year 1996-1997), the net short-wave radiation is the largest positive term (55.5 W m^{-2}), and net all-wave radiation is the main source of energy at the glacier surface (16.5 W m^{-2}), although R does not show any pronounced seasonality. The sensible heat flux (6.0 W m^{-2}) and the conductive heat flux in the snow/ice (2.8 W m^{-2}) also bring energy to the surface. The latent heat flux (-17.7 W m^{-2}) is directed away from the surface which indicates that the surface loses mass by sublimation. An important peculiarity of

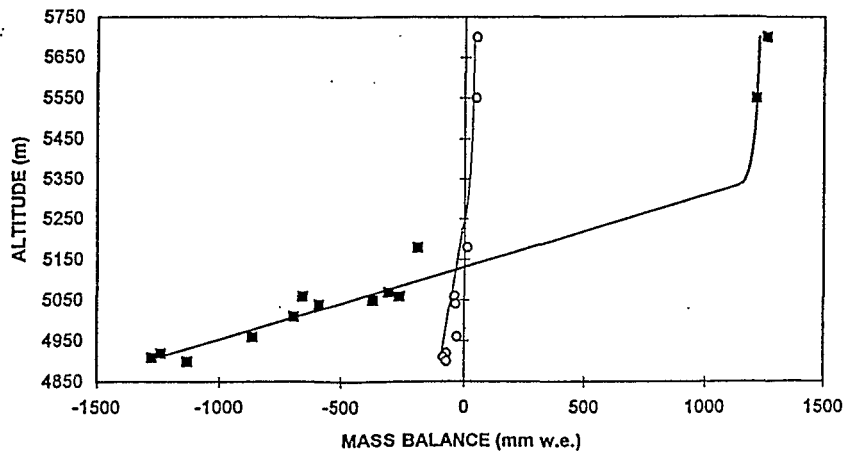


Figure 12. Vertical gradients of mass balance obtained from stake and pit measurements for the wet season (September 1996 to February 1997) (squares) and for the dry season (March 1997 to August 1997) (circles).

tropical glaciers is that the contribution of the latent heat flux to the energy balance is very high and that this energy flux shows a pronounced seasonality, with strong sublimation rates during the dry season and low ones during the humid season. Another peculiarity of these glaciers is the continuously positive sensible heat flux throughout the year, which suggests that the boundary surface layer is almost always in stable conditions. This positive sensible heat flux causes the strong gradient of the vertical net balance profile typical of tropical glaciers in the ablation area.

Albedo, with its direct influence on net all-wave radiation, is the principal factor controlling the amount of energy available at the Zongo Glacier surface, like for every glacier of the world; and humidity, which is responsible for the sharing of the available energy between sublimation and melting, plays the key role to understand the runoff seasonality of the proglacial stream. The high sublimation of the dry season and the absence of precipitation let penitents grow at the glacier surface up to 50 cm high sometimes. The strongly negative latent heat flux characteristic of tropical glaciers makes these glaciers extremely sensitive to climatic changes, like the greenhouse effect for instance. Indeed, they are not only affected by the warming which increases the sensible heat flux but also, and to a bigger extent, by the specific humidity increase which reduces the latent heat flux, saving energy for melting. A better knowledge about tropical glacier functioning is therefore really useful to study the global change. This work already gives a good insight into the annual cycle of the energy balance of a tropical glacier, but the next step in this investigation will be to study the spatial distribution of the surface energy fluxes over the whole glacier.

Acknowledgments. This glaciological program is supported by L'Institut Français de Recherche Scientifique pour le Développement en Coopération (ORSTOM). We are grateful for the assistance received from IHH (Instituto de Hidráulica e Hidrologia), UMSA (Universidad Mayor de San Andrés) in La Paz, and from LGGE (Laboratoire de Glaciologie et Géophysique de l'Environnement) in Grenoble. We received advice from Louis Reynaud, Michel Vallon and Christian Vincent. We thank Johannes Oerlemans, the researchers of the Institute for Marine and Atmospheric Research Utrecht and two anonymous reviewers for making useful comments on earlier versions of the manuscript. The tremendous field work done by J. E. Sicart, J. P. Chazarin, and P. Berton was highly appreciated.

References

- Ambach, W., Nomographs for the determination of meltwater from snow- and ice surfaces, *Ber. Naturwiss. Med. Ver. Innsbruck*, 73, 7-15, 1986.
- Andreas, E. L., A theory for scalar roughness and the scalar transfer coefficient over snow and sea ice, *Boundary Layer Meteorol.*, 38, 159-184, 1986.
- Bintanja, R., and M. Van den Broeke, The surface energy balance of Antarctic snow and blue ice, *J. Appl. Meteorol.*, 34(4), 902-926, 1995.
- Bintanja, R., S. Jonsson, and W. H. Knap, The annual cycle of the surface energy balance of Antarctic blue ice, *J. Geophys. Res.*, 102, 1867-1881, 1997.
- Brutsaert, W., *Evaporation Into the Atmosphere*, 299 pp., D. Reidel, Norwell, Mass., 1982.
- De la Casinière, A. C., Heat exchange over a melting snow surface, *J. Glaciol.*, 13(67), 55-72, 1974.
- Francou, B., P. Ribstein, R. Saravia, and E. Tiriau, Monthly balance and water discharge of an intertropical glacier: Zongo Glacier, Cordillera Real, Bolivia, 16°S, *J. Glaciol.*, 41(137), 61-67, 1995.
- Halberstam, I., and J. P. Schieldge, Anomalous behavior of the atmospheric surface layer over a melting snowpack, *J. Appl. Meteorol.*, 20, 255-265, 1981.
- Hastenrath, S., Heat-budget measurements on the Quelccaya Ice Cap, Peruvian Andes, *J. Glaciol.*, 20(82), 85-97, 1978.
- Hastenrath, S., and A. Ames, Diagnosing the imbalance of Yanamarey Glacier in the Cordillera Blanca of Peru, *J. Geophys. Res.*, 100, 5105-5112, 1995.
- Hastenrath, S., and P. D. Kruss, The role of radiation geometry in the climate response of Mount Kenya's glaciers, 2, Sloping versus horizontal surfaces, *J. Clim.*, 8, 629-639, 1988.
- Hastenrath, S., and P. D. Kruss, The dramatic retreat of Mount Kenya's glaciers between 1963 and 1987: Greenhouse forcing, *Ann. Glaciol.*, 16, 127-133, 1992.
- Hastenrath, S., and J. K. Patnaik, Radiation measurements at Lewis Glacier, Mount Kenya, Kenya, *J. Glaciol.*, 25(93), 439-444, 1980.
- Hense, A., P. Krahe, and H. Flohn, Recent fluctuations of tropospheric temperature and water vapor content in the tropics, *Meteorol. Atmos. Phys.*, 38(4), 215-227, 1988.
- Hock, R., and B. Holmgren, Some aspects of energy balance and ablation of Storglaciären, Northern Sweden, *Geog. Annal.*, 78A, 121-131, 1996.
- Kaser, G., Gletscher in den Tropen, ein Beitrag zur Geographie der tropischen Hochgebirge, in *Habilitationschrift*, 254 pp., Eingereicht bei der Naturwiss. Fak. der Univ. Innsbruck, Austria, 1996.
- Kaser, G., S. Hastenrath, and A. Ames, Mass balance profiles on tropical glaciers, *Z. Gletscherkd. Glazialgeol.*, 32, 75-81, 1996.
- Kotlyakov, V. M., and I. M. Lebedeva, Nieve and ice penitentes: Their way of formation and indicative significance, *Z. Gletscherkd. Glazialgeol.*, X, 111-127, 1974.
- Lliboutry, L., The origin of penitents, *J. Glaciol.* 2(15), 111-127, 1954.
- Lliboutry, L., *Traité de Glaciologie*, 1040 pp., Masson et Cie, Paris, 1964.
- Male, D. H., and R. J. Granger, Snow surface energy exchange, *Water Resour. Res.*, 17(3), 609-627, 1981.
- Marks, D., and J. Dozier, Climate and energy exchange at the snow surface in the alpine region of the Sierra Nevada, 2, Snow cover energy balance, *Water Resour. Res.*, 28(11), 3043-3054, 1992.
- Martin, S., Wind regimes and heat exchange on Glacier de Saint-Sorlin, *J. Glaciol.*, 14(70), 91-105, 1975.
- Meesters, A. G. C. A., N. J. Bink, H. F. Vugts, F. Cannemeijer, and E. A. C. Henneken, Turbulence observations above a smooth melting surface on the Greenland ice sheet, *Boundary Layer Meteorol.*, 85, 81-110, 1997.
- Morris, E. M., Turbulent transfer over snow and ice, *J. Hydrol.*, 105, 205-223, 1989.
- Oké, T. R., *Boundary Layer Climates*, 2nd ed., 435 pp., Routledge, New York, 1987.
- Paterson, W. S. B., *The Physics of Glaciers*, 3rd ed., 477 pp., Pergamon, Tarrytown, N. Y., 1994.
- Plüss, C., *The Energy Balance Over an Alpine Snow Cover*, 115 pp., Geogr. Inst. ETH Zürich, 1997.
- Plüss, C., and R. Mazzoni, The role of turbulent heat fluxes in the energy balance of high alpine snow cover, *Nord. Hydrol.*, 25, 25-38, 1994.
- Ribstein, P., E. Tiriau, B. Francou, and R. Saravia, Tropical climate and glacier hydrology: A case study in Bolivia, *J. Hydrol.*, 165, 221-234, 1995.
- Roché, M. A., A. Aliaga, J. Campos, J. Pena, J. Cortes, and A. Rocha, 'Hétérogénéité des précipitations sur la Cordillère des Andes Boliviennes', in *Hydrology in Mountainous Regions, I, Hydrological Measurements; the Water Cycle*, edited by H. Lang, and A. Musy, *Int. Assoc. Hydrol. Sci. Publ.*, 193, 381-388, 1990.
- Vincent, C., M. Vallon, F. Pinglot, M. Funk, and L. Reynaud, Snow accumulation and ice flow at Dôme du Goûter, Mont Blanc, French Alps, *J. Glaciol.*, 43(145), 513-521, 1997.
- Wagnon, P., P. Ribstein, G. Kaser, and P. Berton, Energy balance and runoff seasonality of a Bolivian glacier, *Global Planet. Change*, in press, 1998.
- B. Francou, ORSTOM, Ap. Post. 17.11.6596, Quito, Ecuador.
- B. Pouyaud, ORSTOM, CP 9214, La Paz, Bolivia.
- P. Ribstein, ORSTOM, UMR Sisyphe, case 123, 4, place Jussieu, 75252 Paris Cedex 05, France.
- P. Wagnon, Laboratoire de Glaciologie et de Géophysique de l'Environnement, 54 rue Molière, BP 96, 38402 Saint Martin d'Hères Cedex, France. (e-mail: patrick@glaciog.ujf-grenoble.fr)

(Received March 14, 1998; revised July 27, 1998; accepted August 26, 1998.)